Detection of Meteor Generated Shock Waves Using the Radio Signatures of Meteor Head Echoes

Reynold E. Silber[1], Wayne K. Hocking[2], Elizabeth A. Silber[3], Maria Gritsevich[4,5]

[1]Department of Earth Sciences, The University of Western Ontario, Canada
[2]Department of Physics and Astronomy, The University of Western Ontario, Canada
[3]Department of Earth, Environmental and Planetary Science, Brown University, USA
[4]Department of Physics, University of Helsinki, Finland
[5]Institute of Physics and Technology, Ural Federal University, Russia

Outline:

- Overdense meteors – fundamentals and shock waves discussion
- MHE – main points

- Using MHE in determination of overdense meteors shock formation altitudes
- Theoretical and technical considerations

- Some aspects of proposed experimental verification
- Conclusion

Overdense Meteors

- Broad term (4×10^{-3} m and up to small-sized fireballs, $q \geq 10^{16}$ electrons m^{-1})

- Statistically small fraction of overall meteoroid influx

- Initial mass loss by sputtering and evaporation by direct atm. molecules collisions

- Each collision $f(v_{meteor})$ may release up to 500 meteoric atoms and ions $\rightarrow$ leads up to the formation of the hydrodynamic shielding ($10^1\, d_{meteor} - 10^2\, d_{meteor}$) (Jenniskens et al., 2000)

- Intense ablation and evaporation driven by high kinetic T and rad. heat transfer (behind the dense shielding)

- Alters the consideration of flow regime, Knudsen number and will push the continuum flow to higher altitudes
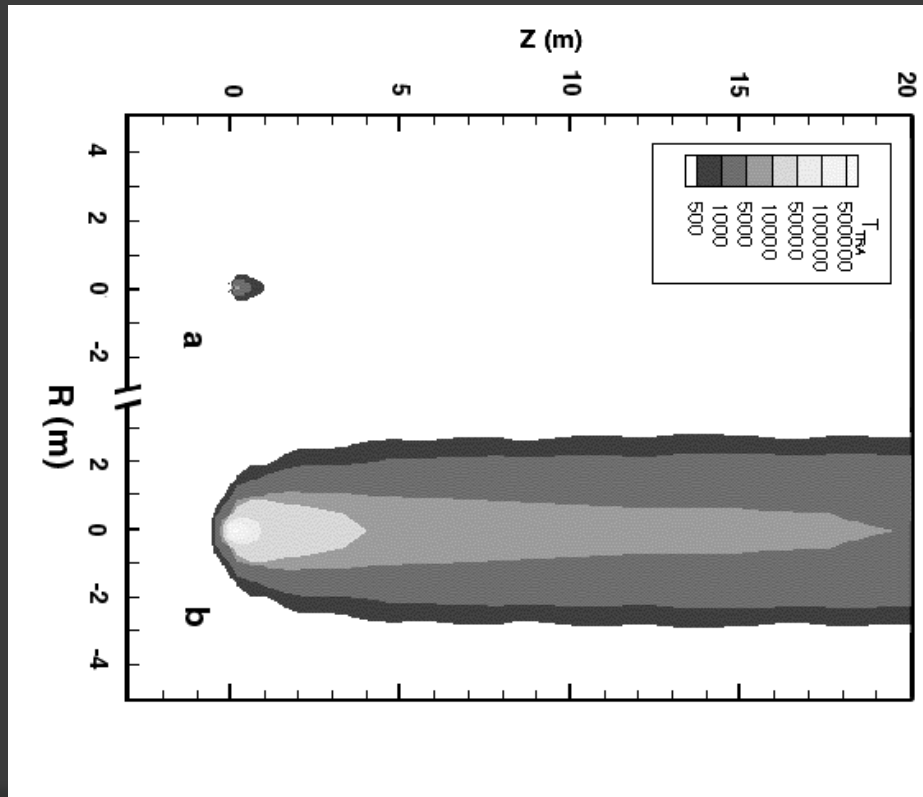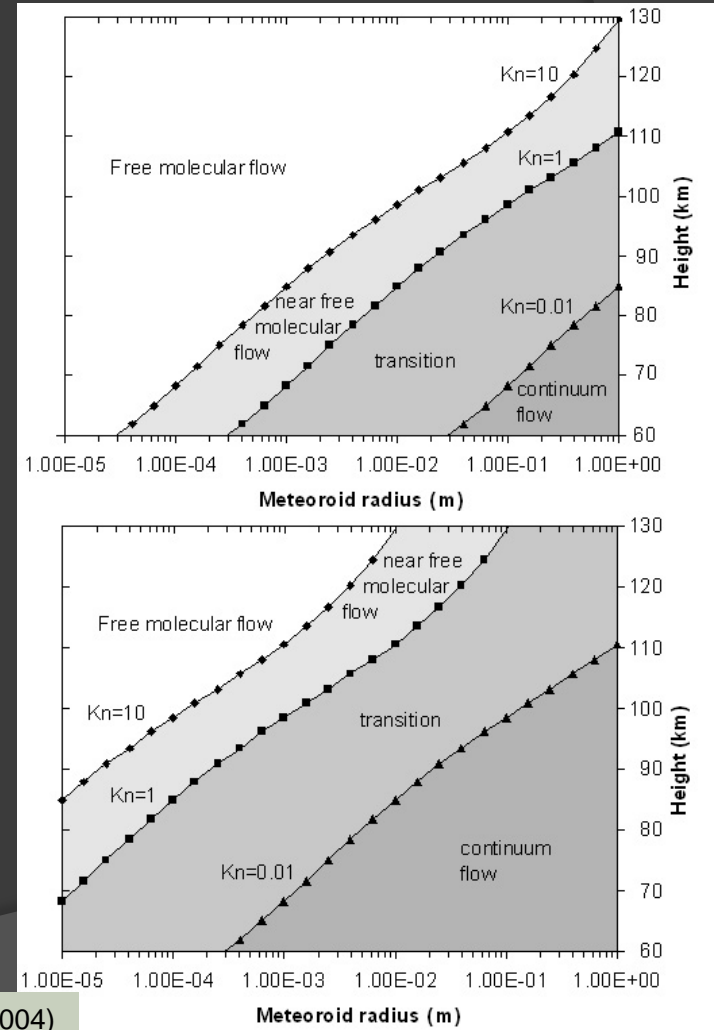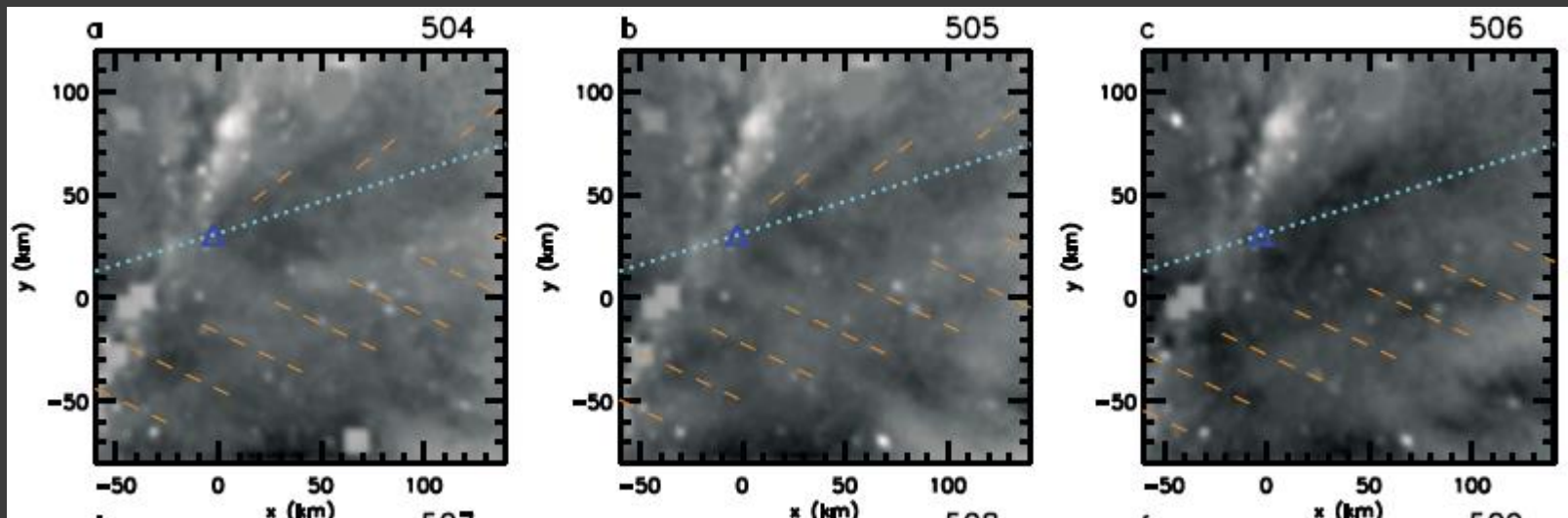

(Jenniskens et al. 2000)   Campbell-Brown & Koschny (2004)

Overdense Meteor Generated Shockwaves in MLT

- Ablation is instrumental for the formation of meteor shock waves (Silber et al. 2017)

- Evidence for cm sized meteoroid generated shockwaves in MLT from infrasonic studies (Silber et al. 2014) and optical observations (gravity waves) (Vadas et al. 2014)


(Vadas et al. 2014)

Shockwaves from Meteors

- More complex than typical shockwaves produced by hypersonic entry vehicles

- Occur when hydrodynamic shielding in front of meteor (vapour cap) gets compressed to such degree that $v, \rho, T,$ gradients between the ambient atmosphere and the hydrodynamic shielding can be treated as discontinuity and obey Rankine-Hugoniot relations (Anderson 2006)
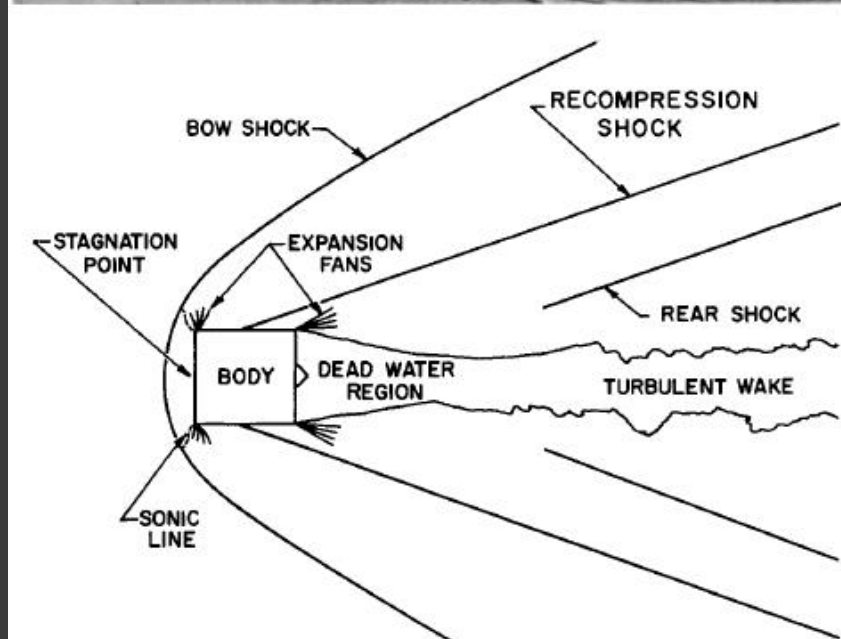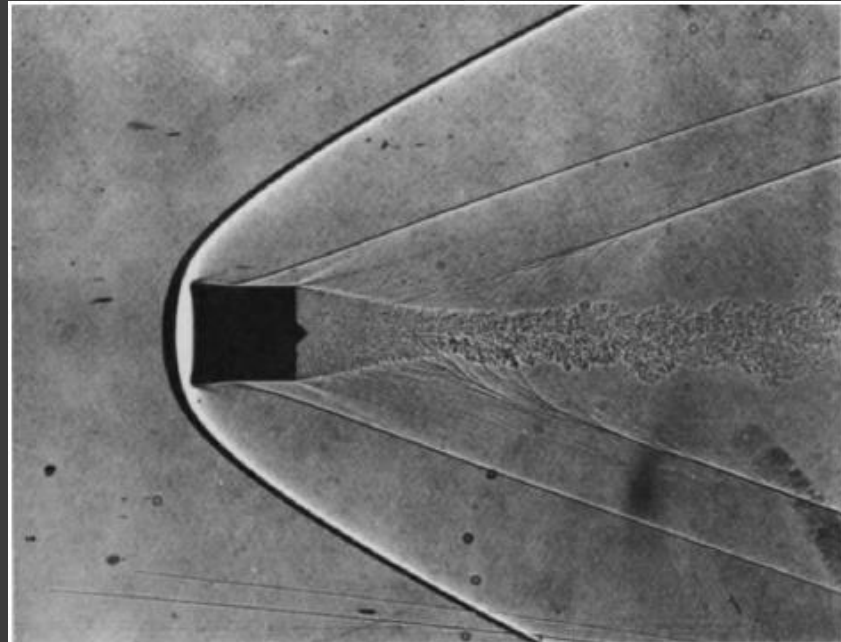
The comparative example of circular cylinder with flat face forward in air a t $M = 3$. (a) Free flight shadowgraph (Ames Aeronautical Laboratory , courtesy National Advisory Committee for Aeronautics) , (b) Sketch of flow field (Hayes and Probstein 1959).

- **Definition:** A shock wave is a discontinuous surface that connects supersonic flow with subsonic flow.

- Behind the shock front, flow velocity is reduced, and P, T and entropy increases across a shock wave (Silber et al. 2017).
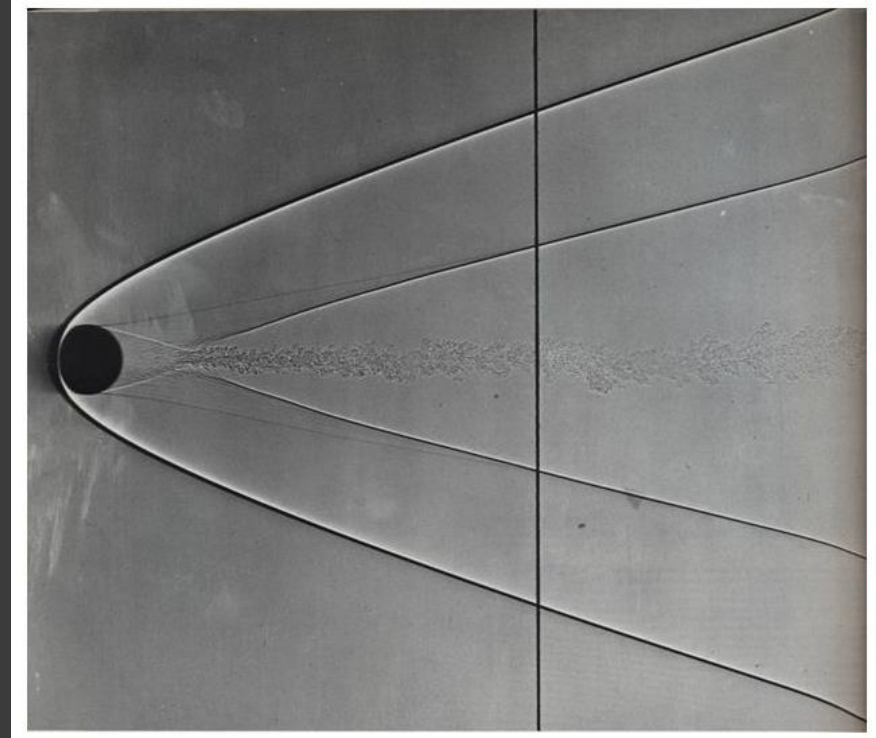
Shadowgraph of 5 cm sphere (M = 4) in free flight through atmospheric air shows boundary layer separation and the formation of the shockwave Credit: A.C. Charters

However we cannot directly observe the formation of overdense meteor generated shock waves, $h(v, d)$ in the region 90 ± 5 km because:

- rapid spatial and temporal attenuation in rarefied atmosphere,
- presence of radiative phenomena
- uncertainty due to ablation-amplified hydrodynamic shielding and its dimensions

- Need a ***tool*** to interpret the formation of coherent flow fields (at specific altitudes) associated with the formation of the meteor generated shock waves in overdense meteors (bow shock envelope)
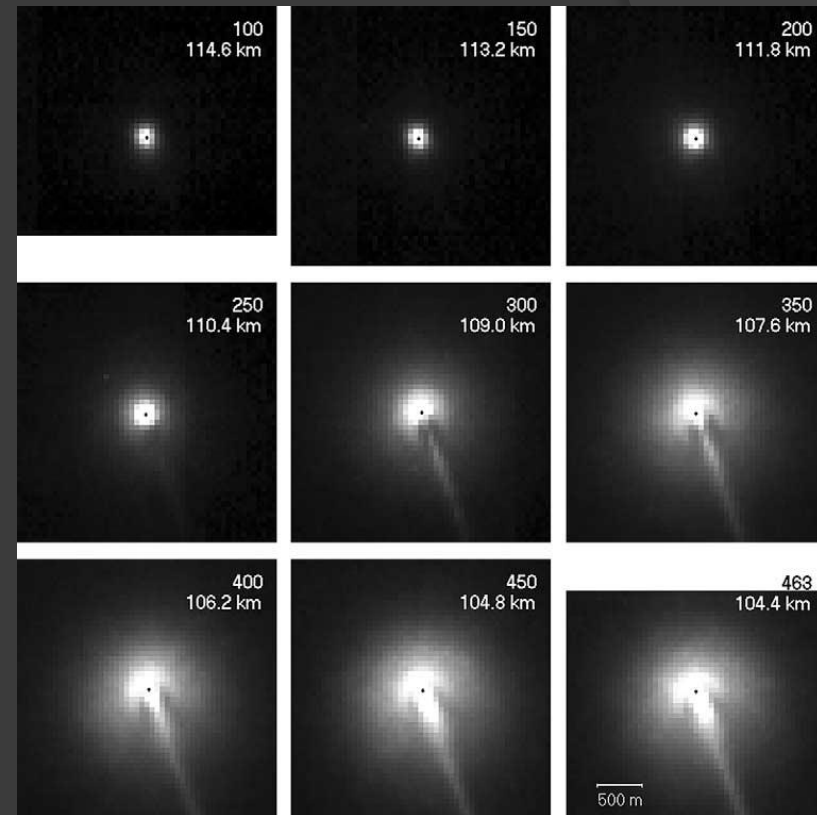
We propose that **MHE** may be used to determine the formation altitude of **overdense** meteor shock waves

How do we define a meteor head echo (MHE)?

(Stenbaek-Nielsen and Jennniskens, 2004)

- ◉ …radar detectable Doppler shifted plasma region that surrounds a meteoroid and travels at its velocity

Images show the development of the shock-like structure during Leonid entry, 115 - 104 km altitudes. In this case it serves as a good visual depiction of the MHE.

- Formation of MHEs coincides with the sputtering regime (colliding atmospheric molecules directly impact the meteoroid surface) - a large number of high energy collisionally evaporated meteoric atoms are ejected – some along the axis of meteor propagation with speeds of up to $1.5 v_{meteor}$.

- Second and third order ionizing collisions of ejected meteoric atoms form fast, scattering high energy electrons, some distance ahead of and around the meteor.

- Coulombic forces ineffective in controlling the departure of high energy ballistic electrons because of the initial charge separation between ions and electrons in the low plasma density (at higher altitudes) .
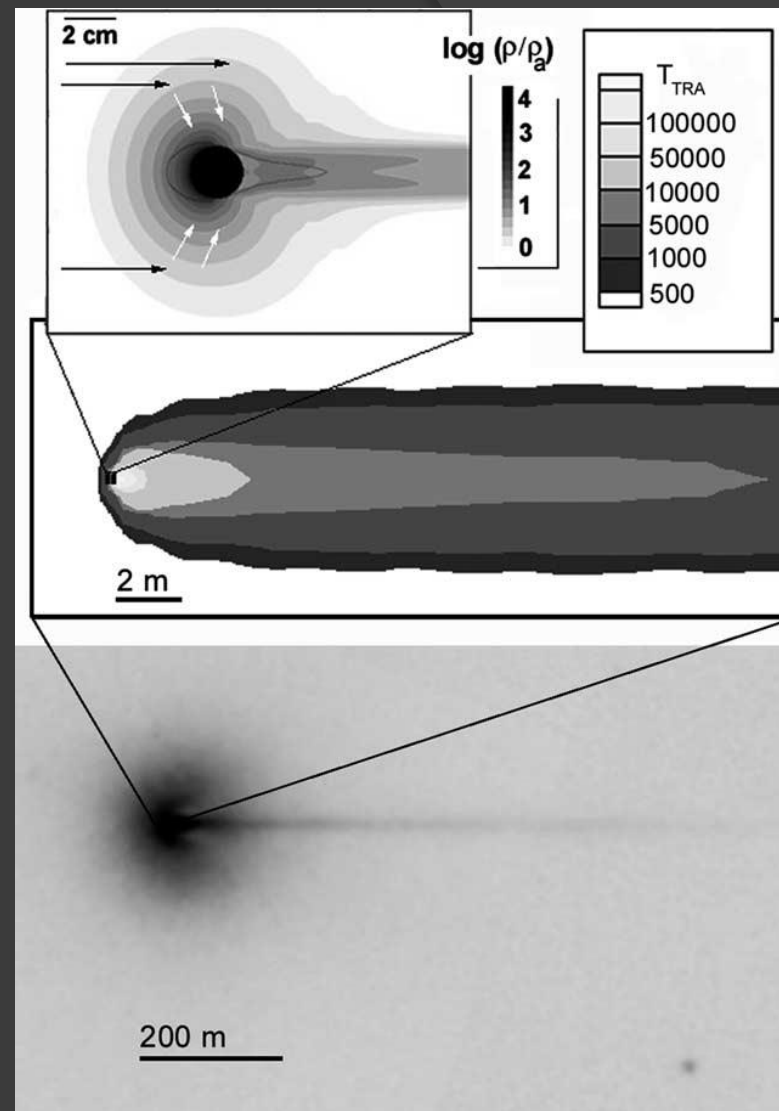
Three scale-sizes of physical phenomena in the Leonid meteor images. Top section of figure shows the meteor vapor cloud calculated by Popova et al., 2000. The center section shows the meteor wake calculated by Boyd, 2000. These models do not describe the "*UV-induced halo and shock-like structure*" seen in the high frame rate imager (bottom). (Stenbaek-Nielsen and Jennniskens, 2004)

Basic Assumptions (e.g. Close et al. 2012)

- MHE region hemispheric – simplifies the interpretation of RCS and the actual geometric area.

- MHE plasma's radius depends upon altitude and scales with the atmospheric mean free path and meteoroid speed

- MHE plasma density - overdense

- At lower altitudes, as the atmospheric mean free path decreases, so will the size of the ionized region

- It is possible to relate those parameters to meteor shock wave formation

How to detect meteor shockwaves and constrain their formation altitudes?

- The MHE will *"terminate" (RCS falls below pre-determined dBsm threshold)* upon the formation of the shock front with high (quasineutral) plasma density in strongly stratified flow fields

- or because its radar RCS will be too small to detect with VHF radar

- In the shock layer and in the region of high plasma density, Coulombic forces are sufficiently strong as to prevent the large scale electron scattering associated with MHEs at higher altitudes.

- $f(\lambda)$ and other set parameters

Shock
Wake
Boundary Layer
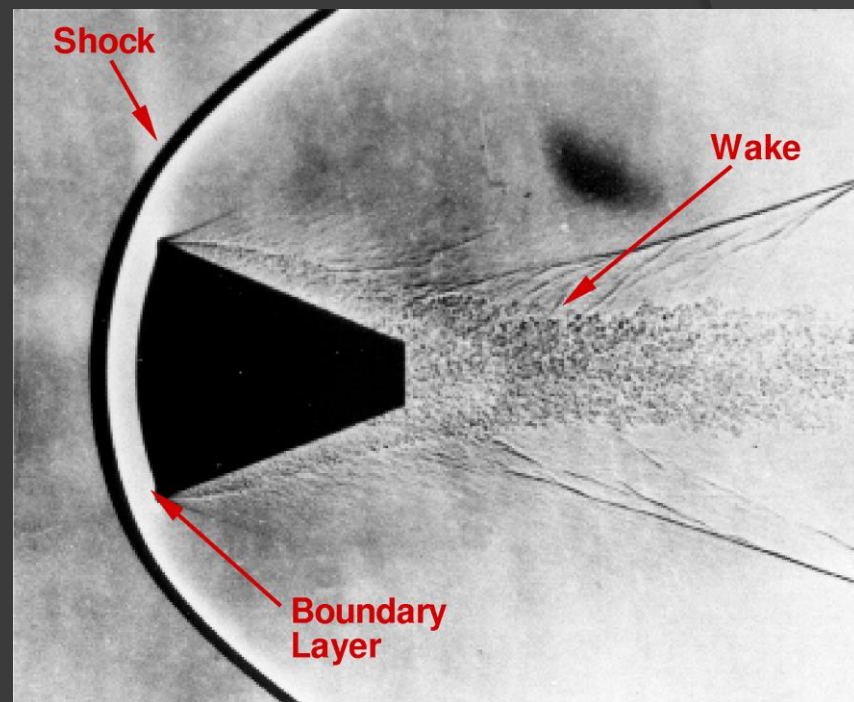
RCS will scale with total number of electrons (e.g. Marshall and Close 2015).

13

Technical Challenges and Considerations

- The observed MHE target sizes strongly depends on the observing radar frequency and associated biases
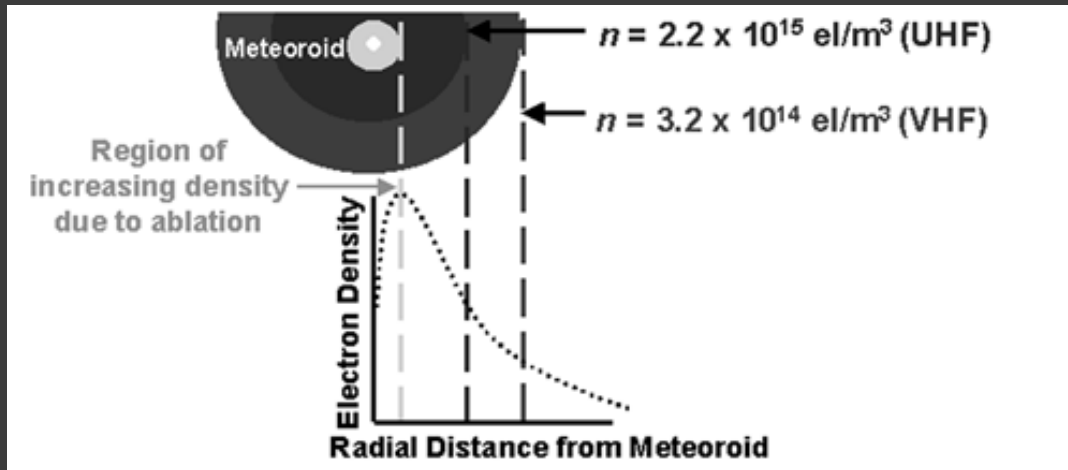

Illustration of how the electron density theoretically varies as a function of distance from the meteoroid. The light colour center represents the meteoroid, the grey portion denotes the region where the electron density increases, and the subsequent dark rings show how the electron density decreases with radius. By assuming overdense reflection, the UHF wave (higher critical frequency) penetrates further into the meteoroid than the VHF reflection, thus explaining the lower UHF RCS (radius of head echo). (Close et al. 2002)

In figure: $n = 2.2 \times 10^{15}$ el/m^3 (UHF); $n = 3.2 \times 10^{14}$ el/m^3 (VHF); Meteoroid; Region of increasing density due to ablation; Electron Density; Radial Distance from Meteoroid

- Target RCS fluctuations due to aspect angle, frequency, and polarization are also present.
- The methodology is simplified by the assumption of hemispherical structure moving at geocentric meteor velocity
- Scattering behaviour function of target circumference and radar wavelength ratio $\alpha = 2\pi a/\lambda$

Experimental Verification

- Should include simultaneous MHE and specular echo from a different and geographically separated system at VHF frequencies
- (*or simultaneous visual observations* e.g. Michell et al. 2015).

Abe et al. 2015
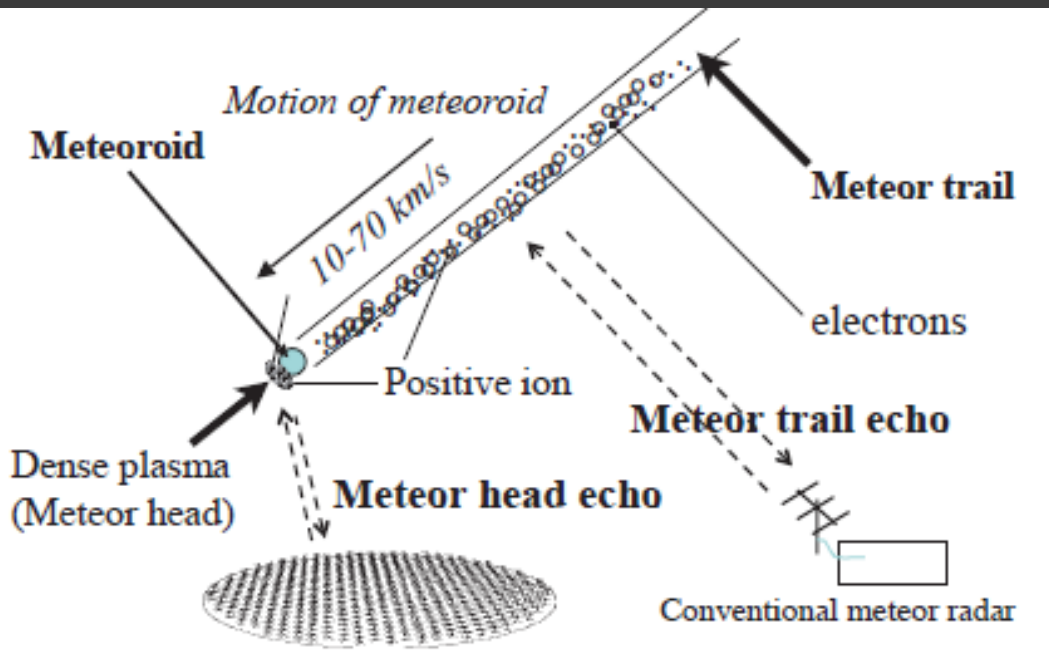
- Exact specular electron line density necessary for exact meteor size determinations

- Actual target size may be different from RCS at different frequencies

- **For a 1 m radius overdense plasma at 20 MHz, $\sigma \approx 0.3$ m^2 which increases to ~3 m^2 at 300 MHz** (Baggaley 2002).

Summary and Conclusions

- We presented theoretical reasoning that MHE may offer valuable tool in constraining the altitudes of shock formation of mm and cm sized overdense meteors.

- The full theoretical treatment is being developed, however the experimental verification is necessary

# Thank you!

# Questions?

Supplemental material

How to detect meteor shockwaves and constrain their formation altitudes? – Cont'd

- **Approach II**: At the altitudes where the size of MHE RCS geometric areas are compatible to the ablationally augmented flow fields around a meteor (generally between 1 and 2 orders of magnitude greater than characteristic meteoroid dimensions (Boyd 2000; Popova et al. 2001), that signifies the existence of strongly stratified density gradients in the plasma layer in front of and around the meteoroid

- This is a direct precursor to the shock wave formation at considered altitude (within uncertainty ± 1 km)

RCS will scale with total number of electrons for plasma radii large compared to the radar wavelength and that this is also proportional to total light production (e.g. Marshall and Close 2015).
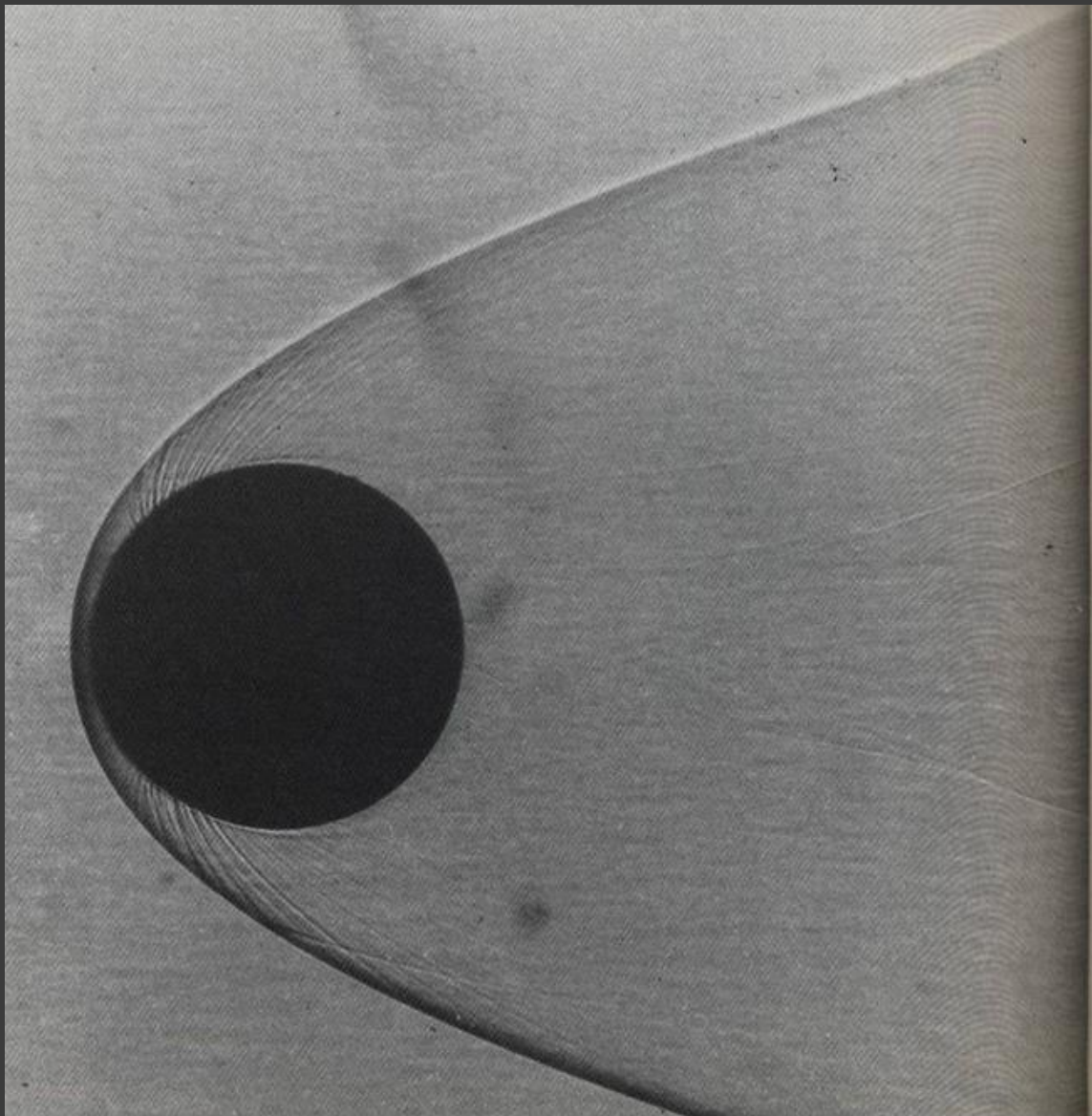
An example of sphere at M = 7.6 flying through atmospheric air. At this marginally high Mach number the bow shock wave is forced closer to the front of the body (bow shock envelope will approach cylindrical shape at Meteor Mach numbers). U.S. Navy photograph from Naval Surface Weapons Center, Silver Springs, Maryland.

Pressure (Pa)

1.0E+03
8.0E+02
6.0E+02
4.0E+02
2.0E+02
0.0E+00
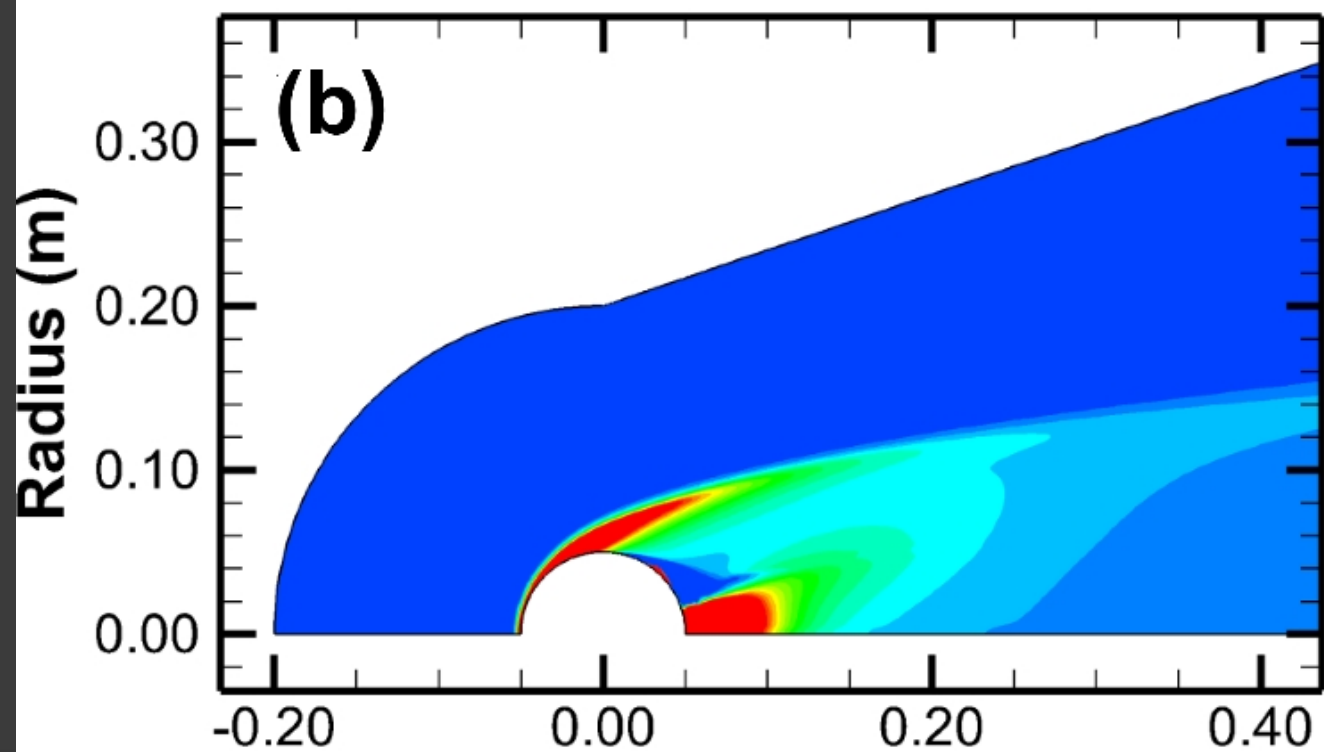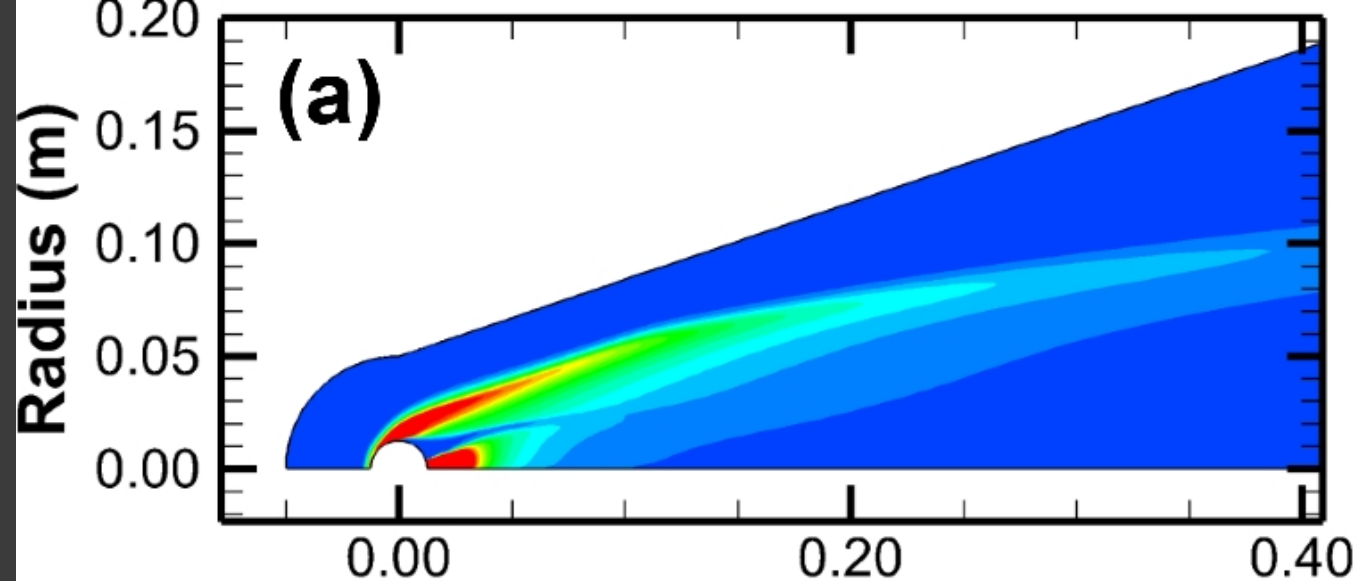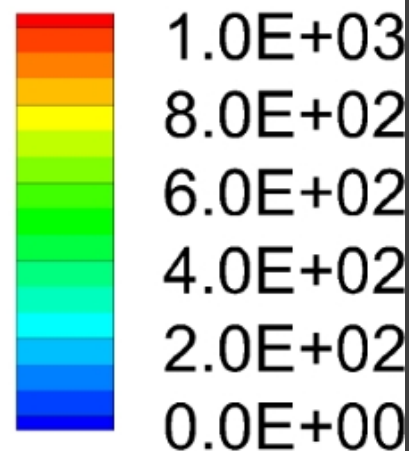
Axial distance (m)
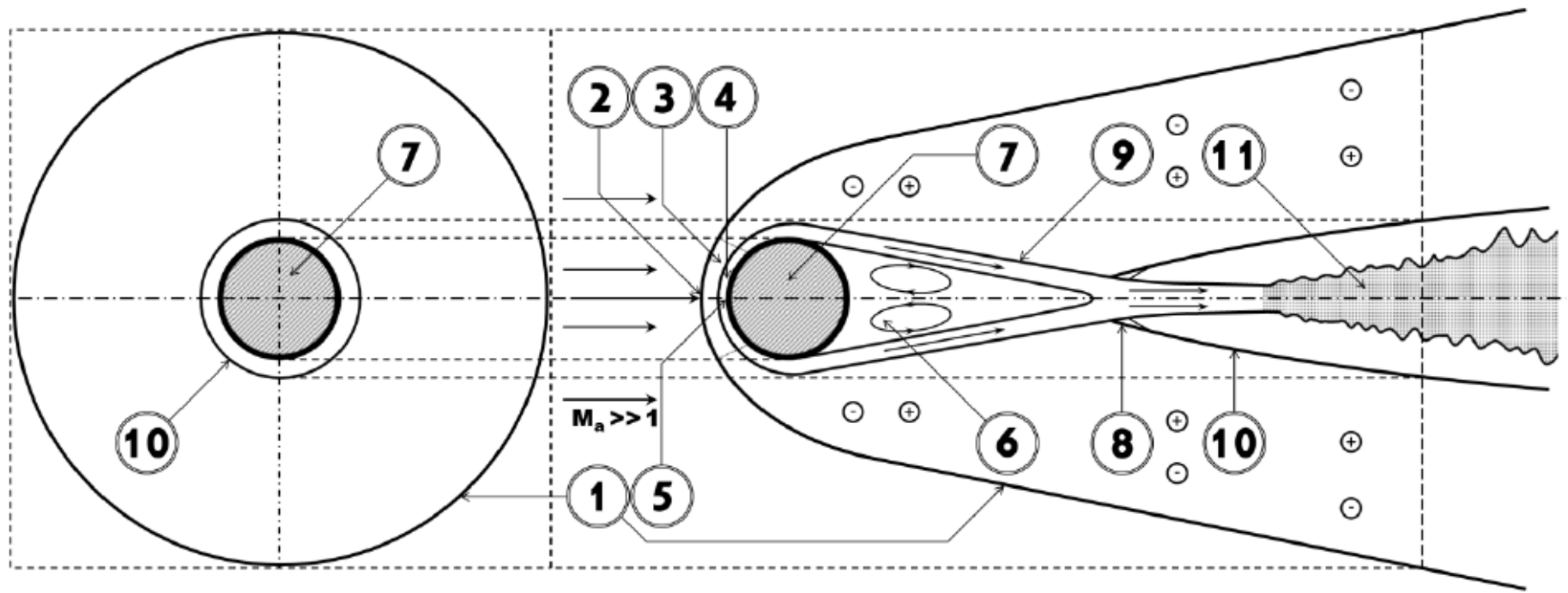
Figure S1: Schematics of the meteor shock wave(s), flow fields and near wake. The meteoroid is considered as a blunt body (with the spherical shape) propagating at hypersonic velocity. The definitions and explanations are provided in the text (after Hayes & Probstein (1959); Lees & Hromas (1961)). (1) Bow (cylindrical) shock wave front; (2) The "ballistic" shock front; (3) Sonic region; (4) Boundary layer; (5) Stagnation point; (6) Turbulent region (in some older literature, this is referred as the dead water region); (7) Meteoroid; (8) The neck and recompression region; (9) The 'free' shear layer; (10) The recompression vapour (or a true cylindrical) shock wave front; (11) The region of turbulent vapour flow and adiabatic expansion. Note that small circles with positive and negative signs indicate regions affected by the presence of ions and electrons respectively. The diagram is only for the illustrative purpose and is not to scale (e.g. for the reasons, see Jenniskens et al. 2000).
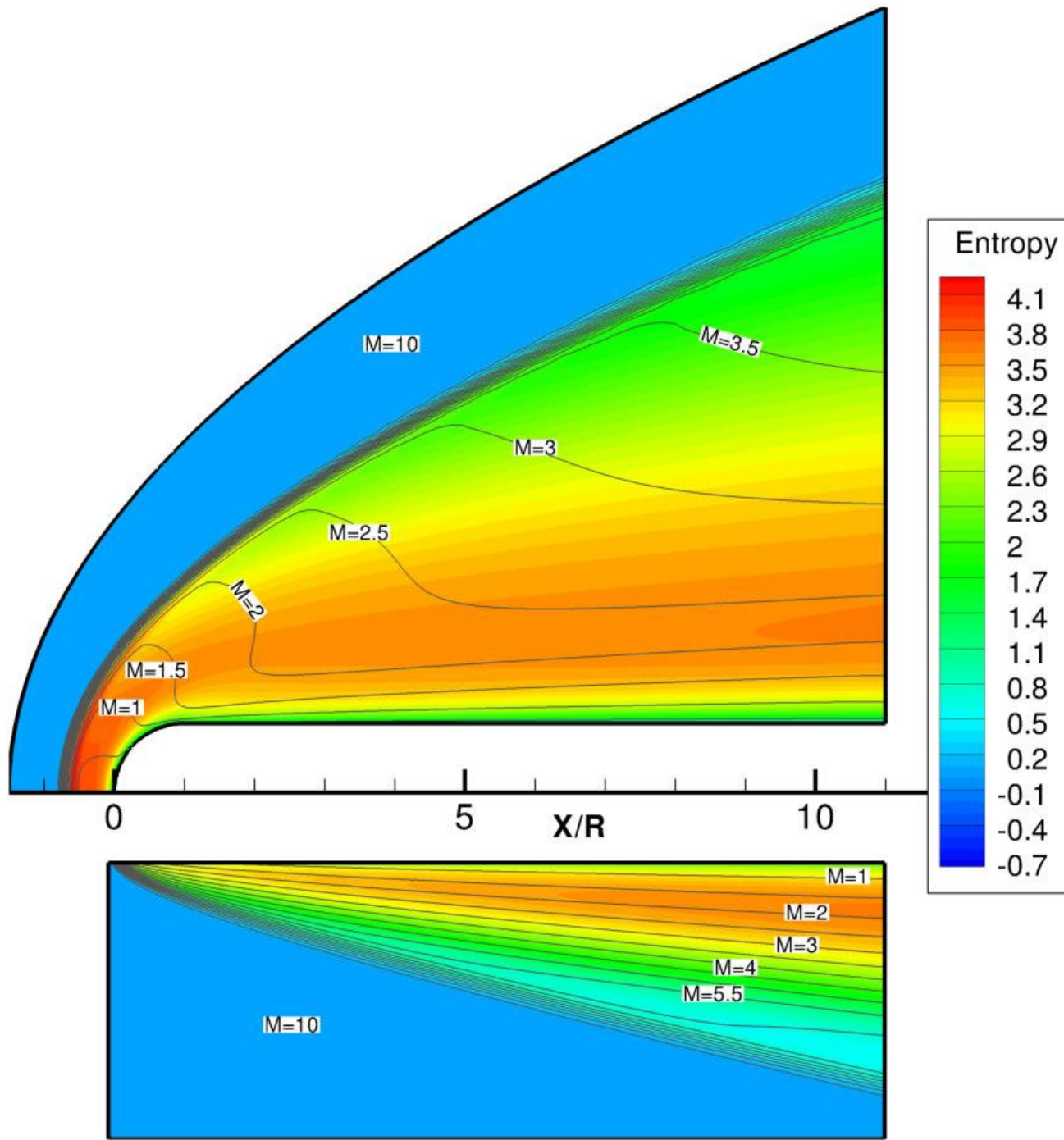
Entropy / Mach number flow fields and y-profiles of temperature and velocity for blunted and sharp plates (NS, M=10).
"Rarefaction and Non-equilibrium Effects in Hypersonic Flows about Leading Edges of Small Bluntness" (Ivanov et al. 2011)

Additional Notes and Supplemental Material

- **x << 1** : Rayleigh scattering
- **x ~ 1** : Mie scattering
- **x >>1** : Geometric scattering

$$x = \frac{2\pi r}{\lambda}$$

- HPLA UHF (930 MHz) – detection limit between 100-80 km = ~ 0.4 cm; VHF (224MHz) detection limit in the same altitude ~1.1 cm

- Rayleigh

- In the frame of reference moving with the meteoroid, the effective mean free path of the evaporated molecules is much shorter than l_∞. They move on the average distance l_r before they collide with an air molecule (Bronshten, 1983):

$$l_r = \frac{v_r}{n_0 v_\infty \sigma_0},$$

$$\alpha = \frac{2\pi a}{\lambda},$$

$$\sigma = \frac{R^4 \left(\frac{S}{N}\right) C}{P_t}$$

where (S/N) is the signal-to-noise ratio (SNR) of the target, R is the range, Pt is the transmitted power, and C is the system calibration constant (contains the Boltzmann constant, bandwidth, system noise temperature, antenna gain and radar wavelength).

If a possible scattering mechanism that may cause head echoes results from coherent returns from a volume of electrons that is small compared with the incident radar wavelength [Mathews et al., 1997] then the backscatter from this volume is proportional to N^2 (number of electrons) according to $\sigma = 4\pi a_o^2 \, N^2$ where a_0 is the classical electron radius.

If a region is to contribute substantially to the RCS its diameter must be less than λ/4; regions outside this will tend to average to the incoherent scatter RCS

Another possibility is overdense scattering [Wannberg et al., 1996], which occurs when the plasma frequency exceeds the radar frequency where f is the incident radar frequency in Hz and n is the electron volume density in cm^3 $\qquad f = 9000\sqrt{n}$

The Mie series can be broken down into three regions: 1. objects that are much less than a wavelength (Rayleigh regime), 2. object sizes that are of the order of the wavelength (resonance region), and 3. objects that are much greater than a wavelength (optical region).

In the Rayleigh regime, where $0 < ka < 1$, the **RCS is proportional to the square of the area of the body** where $k = 2p/\lambda$, a is the Rayleigh radius of the target's cross section and l is the incident wavelength.

$$\frac{\sigma}{\pi a^2} \cong 9\left(\frac{2\pi a}{\lambda}\right)^4$$

- Simplified approach:
- The plasma frequency in overdense MHE (Raleygh regime) greater than λ
- At lower altitudes (below 95 km) the size of plasma region is decreasing with the decreasing atmospheric mean free path.
- The RCS dependence on velocity and altitude revealed a strong correlation between the size of a head echo and the altitude, or mean free path (Close et al. 2002).
- The altitude where the RCS is maximized (105 km)
- Below approx. 100 km, the RCS follows the decrease in the mean free path
- Determination of MHE plasma radius from RCS depends on frequency

Ways to interpret shock wave formation

- Sudden drop in RCS (indicates formation of flow fields where electrons can not escape)
- RCS corresponds to the size of the typical flow field for overdense meteors (1 – 2 orders of magnitude greater than the meteoroid characteristic dimensions).That again indicates the formation of the flow fields.
- Finally, RCS disappears (while meteor is still ablating). That indeed demonstrates the formation of shock fronts and strongly density stratified flow fields. The Coulomb forces are sufficiently strong to control the departure of the energetic electrons. Moreover, large positive ion density will minimize the radar signature and RSC

VISUAL AND RADAR STUDIES OF METEOR HEAD ECHOES

J. JONES

Department of Physics, University of Western Ontario, London, Ont., Canada N6A 3K7

and

A. R. WEBSTER

Department of Electrical Engineering, University of Western Ontario, London, Ont., Canada N6A 5B9

Abstract—Simultaneous visual and radar observations of several of the major meteor showers made over 2 decades have been analysed to determine the conditions favourable for meteor head echoes. We find that the probability of getting a head echo depends quite strongly on range and somewhat less so on the brightness of the meteor. We have shown that the scattering area associated with the head echo varies widely even for meteors of a given meteor shower and that the minimum radius of the equivalent reflecting sphere is of the order of 0.8 m. The distribution of the scattering areas associated with the head echo is approximately a truncated power law whose index varies from shower to shower. An explanation based on the composite meteoroid model of Hawkes and Jones (1975, *Mon. Not. R. astr. Soc.* **173**, 339) is proposed.

In our view the most significant findings of this study are that (i) every visual meteor seems to produce a head echo which however may be too weak to be detected and (ii) the scattering areas associated with the head echoes seem to be distributed approximately as a truncated power law such that the minimum or cut-off scattering area is of the order of somewhat less than 1 m². Both cut-off area and the power law index are shower-dependent. To interpret the results of this
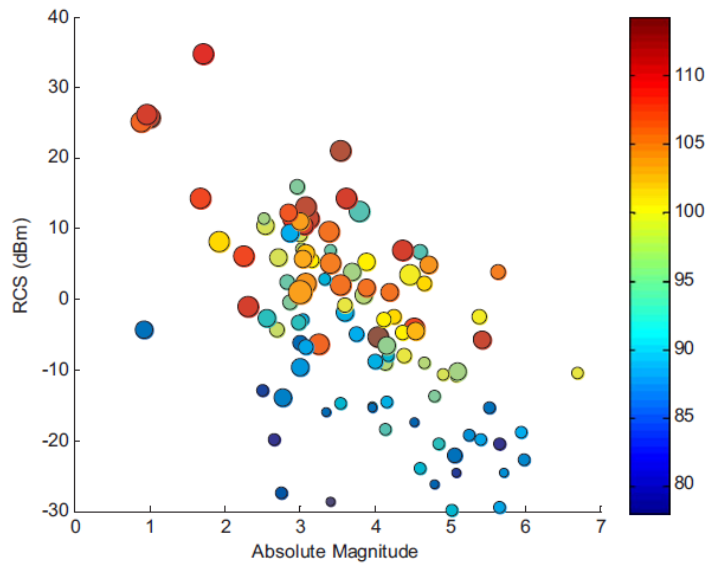
Jones and Webster, (1991)
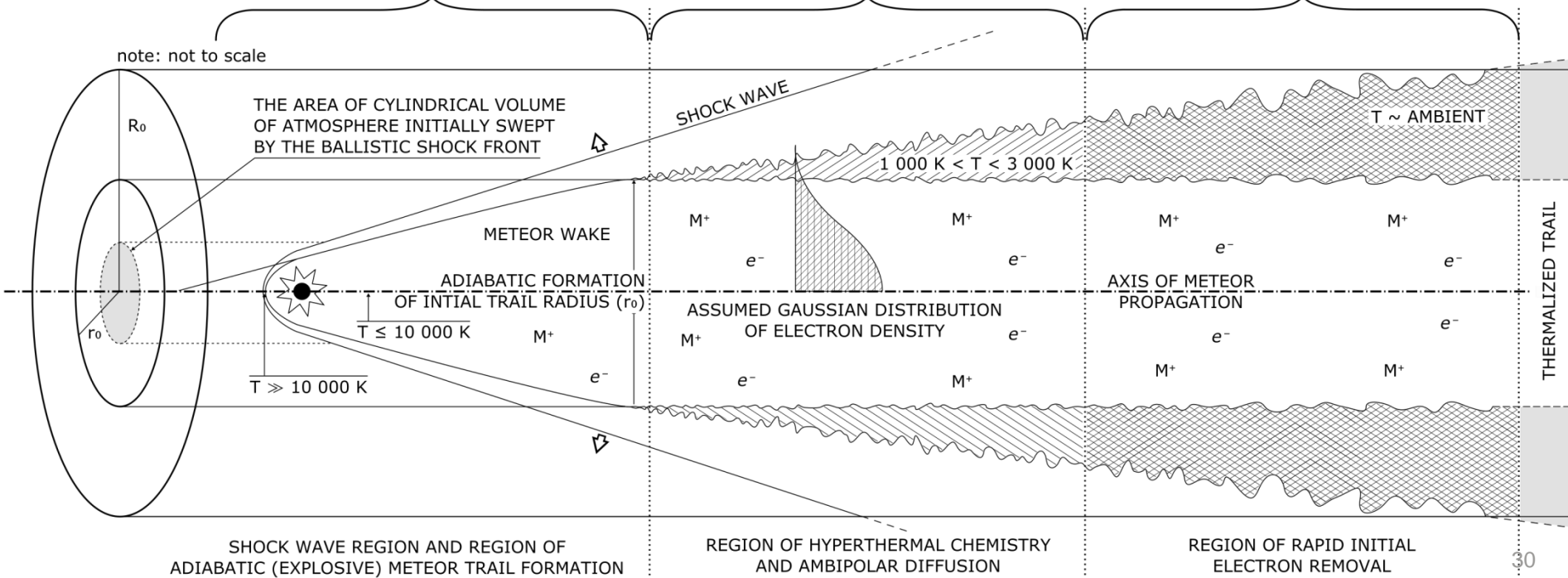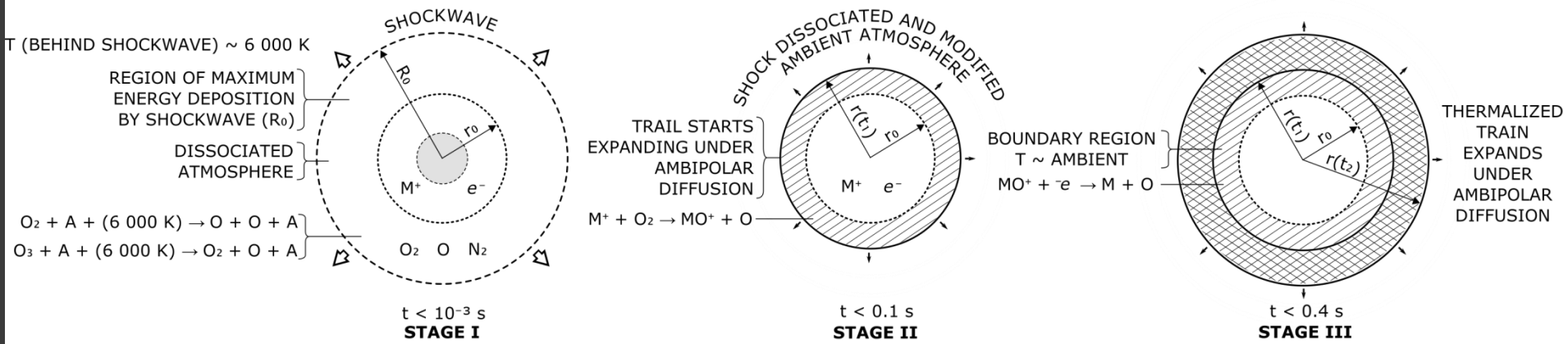
Fig. 9. Peak radar cross section (in units of dB relative to a $1\,m^2$ target) versus the observed magnitude at the same height as the RCS measurement for the head echo with symbol size proportional to speed and color coding by height (in km). (For interpretation of the references to color in this figure legend, the reader is referred to the web version of this article).
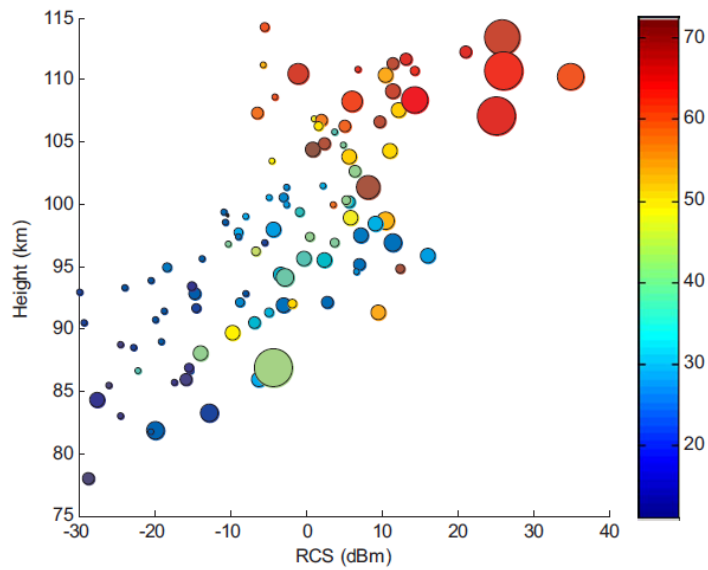

Fig. 10. Height versus peak radar cross section (in units of dB relative to a $1\,m^2$ target) as a function of speed (color coding in km/s) with symbol sizes representing peak meteor absolute brightness in watts. (For interpretation of the references to color in this figure legend, the reader is referred to the web version of this article).
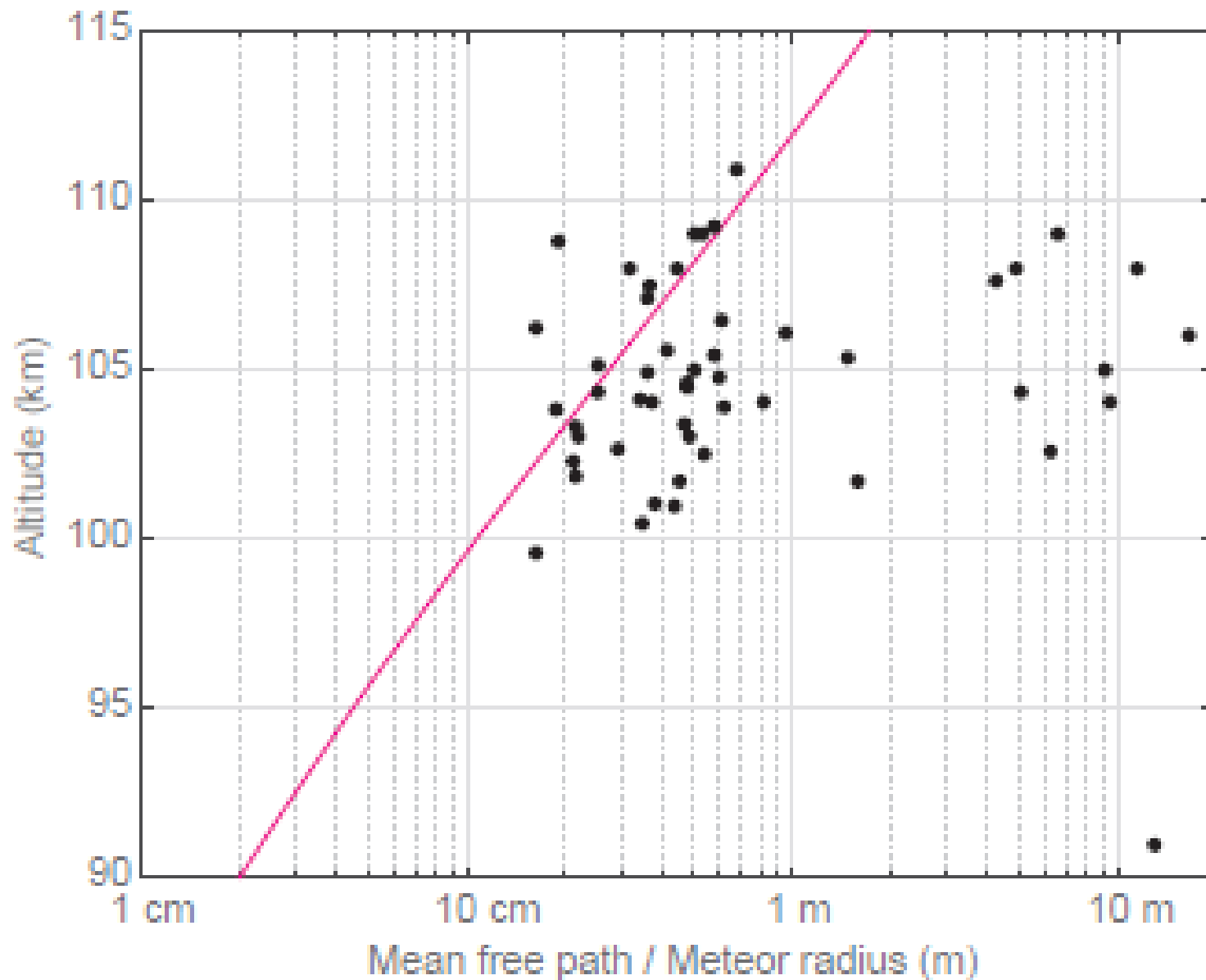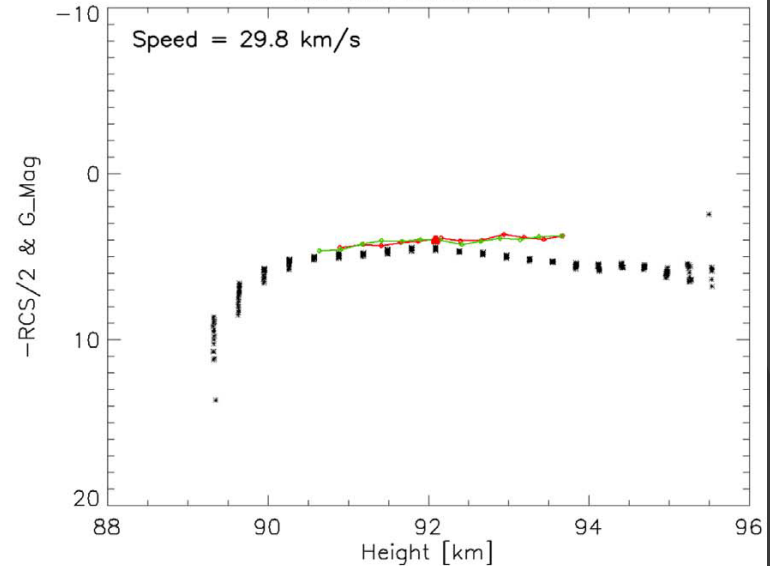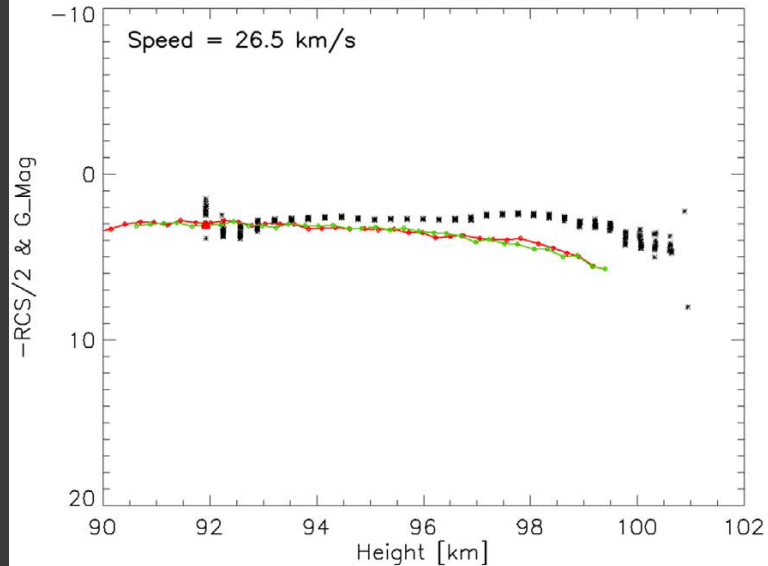
Fig. 6. Mean free path in the upper atmosphere (pink) along with the meteor radii derived using the $1/r^2$ distribution fits. (For interpretation of the references to color in this figure legend, the reader is referred to the web version of this article.)
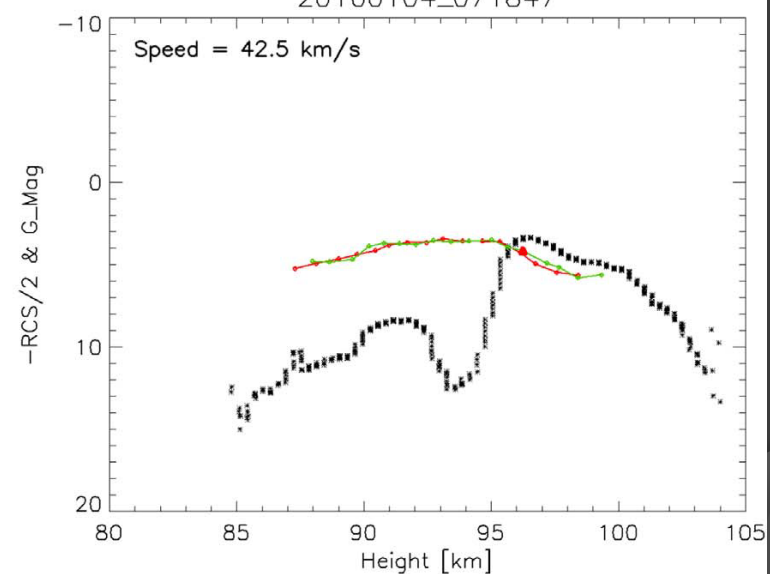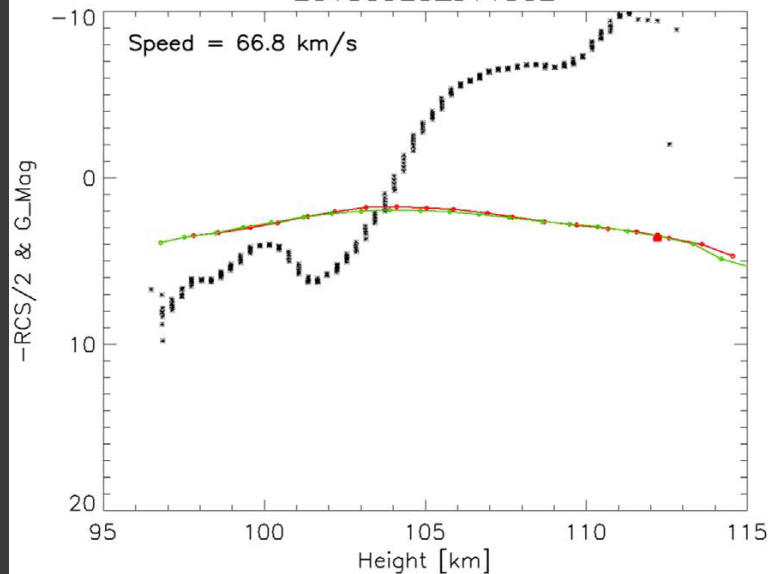
Radar cross section (in units of dB relative to a 1 m² target scaled as –RCS/2 on the y-axis so that larger RCS values are upward) shown as solid black dots versus height for four events. Also shown are the wide field (WATEC) absolute light curves in units of G-band magnitude (y-axis) from the Saura camera (red line) and Alomar (green line). The height on the optical lightcurve where the maximum RCS is reached is shown with a red triangle. The range of y-values is the same for all four events (ranging from 20 dBsm at the top to −40 dBsm at the bottom of the plot). (Brown et al. 2017)